A Review of Single-Phase Grid-Connected Inverters for Photovoltaic Modules

Soeren Baekhoej Kjaer, *Member, IEEE*, John K. Pedersen, *Senior Member, IEEE*, and Frede Blaabjerg, *Fellow, IEEE*

***Abstract*—This review focuses on inverter technologies for connecting photovoltaic (PV) modules to a single-phase grid. The inverters are categorized into four classifications: 1) the number of power processing stages in cascade; 2) the type of power decoupling between the PV module(s) and the single-phase grid; 3) whether they utilizes a transformer (either line or high frequency) or not; and 4) the type of grid-connected power stage. Various inverter topologies are presented, compared, and evaluated against demands, lifetime, component ratings, and cost. Finally, some of the topologies are pointed out as the best candidates for either single PV module or multiple PV module applications.**

***Index Terms*—AC module, photovoltaic (PV) power systems, single-phase grid-connected inverters.**

I. Introduction

PHOTOVOLTAIC (PV) power supplied to the utility grid is gaining more and more visibility, while the world's power demand is increasing [1]. Not many PV systems have so far been placed into the grid due to the relatively high cost, compared with more traditional energy sources such as oil, gas, coal, nuclear, hydro, and wind. Solid-state inverters have been shown to be the enabling technology for putting PV systems into the grid.

The price of the PV modules were in the past the major contribution to the cost of these systems. A downward tendency is now seen in the price for the PV modules due to a massive increase in the production capacity of PV modules. For example, the price per watt for a PV module was between 4.4 $\sim$ 7.9 USD in 1992 and has now decreased to 2.6 $\sim$ 3.5 USD [2]. The cost of the grid-connected inverter is, therefore, becoming more visible in the total system price. A cost reduction per inverter watt is, therefore, important to make PV-generated power more attractive [4]. Focus has, therefore, been placed on new, cheap, and innovative inverter solutions, which has resulted in a high diversity within the inverters, and new system configurations.

This paper starts with an examination of the demands for the inverters, set up by utility grid companies, the PV modules, and the operators. This is followed by a historical review to see how these demands were achieved in the past, how they are reached today, and perhaps how they will be realized in the future. Next follows an overview of some existing power inverter topologies for interfacing PV modules to the grid. The approaches are further discussed and evaluated in order to recognize the most suitable topologies for future PV inverters, and, finally, a conclusion is given.

Paper IPCSD-05-002, presented at the 2002 Industry Applications Society Annual Meeting, Pittsburgh, PA, October 13–18, and approved for publication in the IEEE Transactions on Industry Applications by the Industrial Power Converter Committee of the IEEE Industry Applications Society. Manuscript submitted for review March 1, 2004 and released for publication June 16, 2005.

S. B. Kjaer is with PowerLynx A/S, DK-6400 Sønderborg, Denmark (e-mail: sbk@powerlynx.com; sbkjaer@ieee.org).

J. K. Pedersen and F. Blaabjerg are with the Institute of Energy Technology, Aalborg University, DK-9220 Aalborg East, Denmark (e-mail: jkp@iet.aau.dk; fbl@iet.aau.dk).

Digital Object Identifier 10.1109/TIA.2005.853371

II. Specifications, Demands, and Standards

Inverter interfacing PV module(s) with the grid involves two major tasks. One is to ensure that the PV module(s) is operated at the maximum power point (MPP). The other is to inject a sinusoidal current into the grid. These tasks are further reviewed in this section.

A. Demands Defined by the Grid

Since the inverter is connected to the grid, the standards given by the utility companies must be obeyed. In particular, the future international standard (still a Committee Draft for Vote-CDV) IEC61727 [3] and the present standards EN61000-3-2 [4], IEEE1547 [5] and the U.S. *National Electrical Code* (NEC) 690 [6] are worth considering. These standards deal with issues like power quality, detection of islanding operation, grounding, etc. Summaries are listed in Table I.

As seen in Table I, the present EN standard (applied in Europe) is easier to cope with, regarding current harmonics, than the corresponding IEEE and IEC standards. This is also reflected in the chosen inverter topologies, which have changed from large thyristor-equipped grid-connected inverters to smaller insulated-gate-bipolar-transistor (IGBT)/MOSFET-equipped ones.

The inverters must also be able to detect an islanding situation, and take appropriate measures in order to protect persons and equipment [7]. Islanding is the continued operation of the inverter when the grid has been removed on purpose, by accident, or by damage. In other words, the grid has been removed from the inverter, which then only supplies local loads. The available detection schemes are normally divided into two groups: active and passive. The passive methods do not have any influence on the power quality, since they just monitor grid parameters. The active schemes introduce a disturbance into the grid and monitor the effect. This may affect the power quality, and problems with multiple inverters in parallel with the grid are also known to exist [7], [8].

The IEEE [5] and the IEC [3] standards put limitations on the maximum allowable amount of injected dc current into the grid. The purpose of limiting the injection is to avoid saturation of the distribution transformers [7]. However, the

0093-9994/$20.00 © 2005 IEEE

APsystems Ex. 1008
Altenergy Power Sys. v. CyboEnergy
IPR2024-00362
Page 00001

TABLE I
SUMMARY OF THE MOST INTERESTING STANDARDS DEALING WITH INTERCONNECTIONS OF PV SYSTEMS TO THE GRID

ISSUE	IEC61727 [3]	IEEE1547 [5]	EN61000-3-2 [4]
Nominal power	10 kW	30 kW	16 A × 230 V = 3.7 kW
Harmonic currents (Order – h) Limits	(3-9) 4.0% (11-15) 2.0% (17-21) 1.5% (23-33) 0.6%	(2-10) 4.0% (11-16) 2.0% (17-22) 1.5% (23-34) 0.6% (> 35) 0.3%	(3) 2.30 A (5) 1.14 A (7) 0.77 A (9) 0.40 A (11) 0.33 A (13) 0.21 A (15-39) 2.25/h
	Even harmonics in these ranges shall be less than 25% of the odd harmonic limits listed.		Approximately 30% of the odd harmonics -see standard.
Maximum current THD	5.0%		-
Power factor at 50% of rated power	0.90	-	
DC current injection	Less than 1.0% of rated output current.	Less than 0.5% of rated output current.	< 0.22 A -corresponds to a 50 W half-wave rectifier.
Voltage range for normal operation	85% - 110% (196 V – 253 V)	88% - 110% (97 V – 121 V)	-
Frequency range for normal operation	50 ± 1 Hz	59.3 Hz to 60.5 Hz	-

limits are rather small (0.5% and 1.0% of rated output current), and such small values can be difficult to measure precisely with the exciting circuits inside the inverters. This can be mitigated with improved measuring circuits or by including a line-frequency transformer between the inverter and the grid. Some inverters use a transformer embedded in a high-frequency dc–dc converter for galvanic isolation between the PV modules and the grid. This does not, however, solve the problem with dc injection, but makes the grounding of the PV modules easier.

The NEC 690 standard [6] demands that the PV modules shall be system grounded and monitored for ground faults, when the maximum output voltage of the PV modules reaches a certain level, e.g., 50 V [6], [7], [26]. System ground involves the negative (positive) terminal of the PV array(s) being connected to ground. This can be troublesome for many high-power transformerless systems, since a single-phase inverter with neutral-to-line grid connection already is system grounded on the grid side. Other Electricity Boards only demand equipment ground of the PV modules in the case of absent galvanic isolation [7], [9]. Equipment ground is the case when frames and other metallic parts are connected to ground.

Assuming that both the grid voltage and grid current only contain the fundamental component and that they are in phase, the instantaneous power injected into the grid becomes equal to

$$p_{\text{grid}} = 2 \cdot P_{\text{grid}} \cdot \sin^2(\omega_{\text{grid}} \cdot t) \tag{1}$$

where P_{grid} is the average injected power, ω_{grid} is the angular frequency, and t is time.

B. Demands Defined by the Photovoltaic Module(s)

A model of a PV cell is sketched in Fig. 1(a), and its electrical characteristic is illustrated in Fig. 1(b). The most common PV technologies nowadays are the monocrystalline- and the multicrystalline-silicon modules, which are based on traditional, and expensive, microelectronic manufacturing processes [1]. The MPP voltage range for these PV modules is normally defined in the range from 23 to 38 V at a power generation of approximate 160 W, and their open-circuit voltage is below 45 V. However, new technologies like thin-layer silicon, amorphous-silicon, and hoto Electro Chemical (PEC) are in development [1], [10]. These types of PV modules can be made arbitrarily large by an inexpensive "roll-on–roll-off" process.

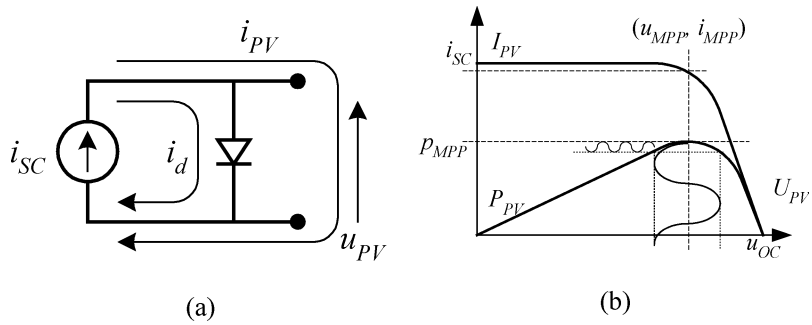

Fig. 1. Model and characteristics of a PV cell. (a) Electrical model with current and voltages defined. (b) Electrical characteristic of the PV cell, exposed to a given amount of (sun)light at a given temperature. As indicated, ripple at the PV module's terminals results in a somewhat lower power generation, compared with the case where no ripple is present at the terminals.

This means that new modules with only one cell may see the light in the future. The voltage range for these cells/modules is located around 0.5 $\sim$ 1.0 V at several hundred amperes per square meter cell [11]–[13].

The inverters must guarantee that the PV module(s) is operated at the MPP, which is the operating condition where the most energy is captured. This is accomplished with an MPP tracker (MPPT). It also involves the ripple at the terminals of the PV module(s) being sufficiently small, in order to operate around the MPP without too much fluctuation. Analyses of the circuit in Fig. 1(a) show that there is a relationship between the amplitude of the voltage ripple and the utilization ratio K_{PV}, given as [14]

$$\hat{u} = \sqrt{\frac{(k_{\mathrm{PV}} - 1) \cdot 2 \cdot P_{\mathrm{MPP}}}{3 \cdot \alpha \cdot U_{\mathrm{MPP}} + \beta}} = 2 \cdot \sqrt{\frac{(k_{\mathrm{PV}} - 1) \cdot P_{\mathrm{MPP}}}{\frac{d^2 p_{\mathrm{PV}}}{d u_{\mathrm{PV}}^2}}} \quad (2)$$

where $\hat{u}$ is the amplitude of the voltage ripple, P_{MPP} and $\mathrm{U}_{\mathrm{MPP}}$ are the power and voltage at the MPP, α and β are the coefficients describing a second-order Taylor approximation of the current, and the utilization ratio is given as the average generated power divided by the theoretical MPP power. The coefficients are computed as

$$i_{\mathrm{PV}} = \alpha \cdot u_{\mathrm{PV}}^2 + \beta \cdot u_{\mathrm{PV}} + \gamma \quad (3)$$

$$u_{\mathrm{PV}} \approx U_{\mathrm{MPP}} + \hat{u} \cdot \sin(\omega \cdot t) \quad (4)$$

$$\alpha = \frac{1}{2} \cdot \frac{d^2 I_{\mathrm{MPP}}}{d U_{\mathrm{MPP}}^2} \quad (5)$$

$$\beta = \frac{d I_{\mathrm{MPP}}}{d U_{\mathrm{MPP}}} - 2 \cdot \alpha \cdot U_{\mathrm{MPP}} \quad (6)$$

$$\gamma = \alpha \cdot U_{\mathrm{MPP}}^2 - \frac{d I_{\mathrm{MPP}}}{d U_{\mathrm{MPP}}} \cdot U_{\mathrm{MPP}} + I_{\mathrm{MPP}}. \quad (7)$$

Calculations show that the amplitude of the ripple voltage should be below 8.5% of the MPP voltage in order to reach a utilization ratio of 98%. For example, a PV module with an MPP voltage of 35 V should not be exposed to a voltage ripple of more than 3.0 V (amplitude), in order to have a utilization ratio of 98%. As seen in the previous section, the power injected into the grid follows a sinusoidal wave, raised to the second power, $[\sin^2(\omega \cdot t)]$, for which reason the inverter must contain a power decoupling device.

C. Demands Defined by the Operator

The operator (the owner) also has a few words to say. First of all, the inverter must be cost effective, which is easily achieved with similar circuits as these used in today's single-phase power-factor-correction (PFC) circuits and variable-speed drives (VSDs). However, the user also demands a high efficiency over a wide range of input voltage and input power since these variables are defined in very wide ranges as functions of solar irradiation and ambient temperature. Fig. 2 shows the average irradiation during a normal year in Denmark (Northwestern Europe) [15]. The figure shows that most of the potential energy is available in the range from 50 to 1000 W/m^2 of irradiation.

Further, the inverter must be highly reliable (long operational lifetime) since most PV module manufacturer offer a warranty of 25 years on 80% of initial efficiency, and a materials and workmanship warranty of five years [27].

The main limiting components inside the inverters are the electrolytic capacitors used for power decoupling between the PV module and the single-phase grid [16]–[19]. The operational lifetime for electrolytic capacitors is given by [20]

$$L_{\mathrm{OP}} = L_{\mathrm{OP},0} \cdot 2^{\left(\frac{T_0 - T_h}{\Delta T}\right)} \quad (8)$$

where L_{OP} is the operational lifetime, $L_{\mathrm{OP},0}$ is the lifetime at a hotspot temperature of T_0, T_h is the hotspot temperature, and ΔT is the temperature increase which reduces the lifetime by a factor of two. However, the equation assumes a constant temperature, which can be approximated when the inverter is placed indoors and neglecting the power loss inside the capacitor, but certainly not when the inverter is integrated with the PV module, as for the ac module. In the case of a varying temperature a mean value of (8) must be applied to determine the lifetime [20].

III. Evolution of PV Inverters

A. The Past—Centralized Inverters

The past technology, illustrated in Fig. 3(a), was based on centralized inverters that interfaced a large number of PV modules to the grid [25]. The PV modules were divided into series connections (called a string), each generating a sufficiently high voltage to avoid further amplification. These series connections were then connected in parallel, through string diodes, in order to reach high power levels. This centralized inverter includes

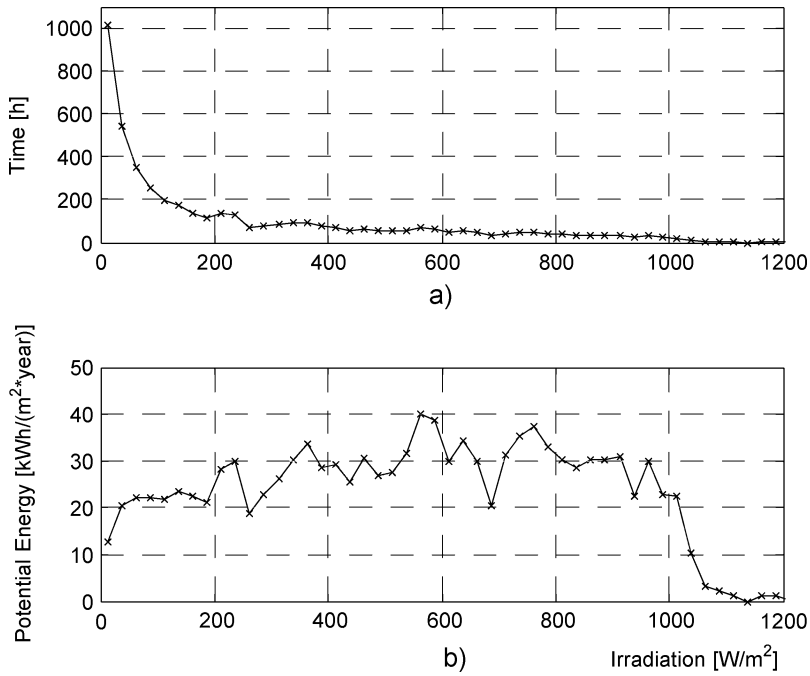

Fig. 2. Meteorological data. (a) Irradiation distribution for a Danish reference year. (b) Solar energy distribution for a Danish reference year. Total time of irradiation equals 4686 h per year. Total potential energy is equal to 1150 $\mathrm{kWh}/(\mathrm{m}^2 \cdot \mathrm{y}) \approx 130\ \mathrm{W/m}^2$ [15].

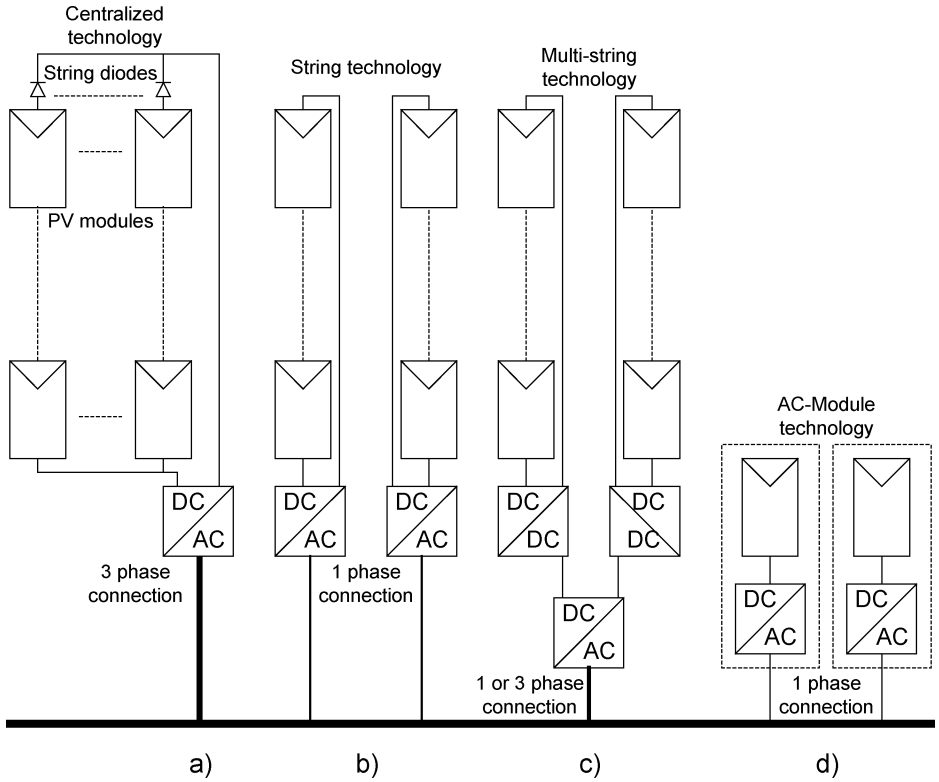

Fig. 3. Historical overview of PV inverters. (a) Past centralized technology. (b) Present string technology. (c) Present and future multi-string technology. (d) Present and future ac-module and ac cell technologies.

some severe limitations, such as high-voltage dc cables between the PV modules and the inverter, power losses due to a centralized MPPT, mismatch losses between the PV modules, losses in the string diodes, and a nonflexible design where the benefits of mass production could not be reached. The grid-connected stage was usually line commutated by means of thyristors, involving many current harmonics and poor power quality. The large amount of harmonics was the occasion of new inverter topologies and system layouts, in order to cope with the emerging standards which also covered power quality.

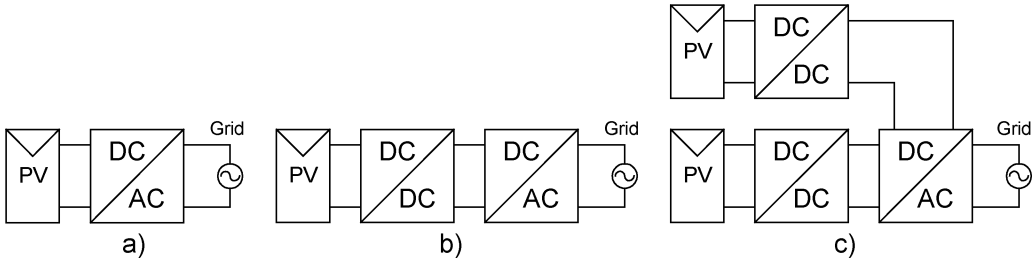

Fig. 4. Three types of PV inverters. Please note that the sign for the PV module shall be interpreted as either a single PV module, or as multiple PV modules in series/parallel connections. (a) A single power processing stage that handles the MPPT, voltage amplification, and grid current control. (b) Dual power processing inverter where the dc–dc converter is responsible for the MPPT and the dc–ac inverter controls the grid current. Voltage amplification can be included in both stages. (c) Dual-stage inverter, where each PV module or string is connected to a dedicated dc–dc converter that is connected to a common dc–ac inverter.

B. The Present—String Inverters and AC Modules

The present technology consists of the string inverters and the ac module [25]. The string inverter, shown in Fig. 3(b), is a reduced version of the centralized inverter, where a single string of PV modules is connected to the inverter [7]. The input voltage may be high enough to avoid voltage amplification. This requires roughly 16 PV modules in series for European systems. The total open-circuit voltage for 16 PV modules may reach as much as 720 V, which calls for a 1000-V MOSFET/IGBT in order to allow for a 75% voltage de-rating of the semiconductors. The normal operation voltage is, however, as low as 450 $\sim$ 510 V. The possibility of using fewer PV modules in series also exists, if a dc–dc converter or line-frequency transformer is used for voltage amplification. There are no losses associated with string diodes and separate MPPTs can be applied to each string. This increases the overall efficiency compared to the centralized inverter, and reduces the price, due to mass production.

The ac module depicted in Fig. 3(d) is the integration of the inverter and PV module into one electrical device [7]. It removes the mismatch losses between PV modules since there is only one PV module, as well as supports optimal adjustment between the PV module and the inverter and, hence, the individual MPPT. It includes the possibility of an easy enlarging of the system, due to the modular structure. The opportunity to become a "plug-and-play" device, which can be used by persons without any knowledge of electrical installations, is also an inherent feature. On the other hand, the necessary high voltage-amplification may reduce the overall efficiency and increase the price per watt, because of more complex circuit topologies. On the other hand, the ac module is intended to be mass produced, which leads to low manufacturing cost and low retail prices.

The present solutions use self-commutated dc–ac inverters, by means of IGBTs or MOSFETs, involving high power quality in compliance with the standards.

C. The Future—Multi-String Inverters, AC Modules, and AC Cells

The multi-string inverter depicted in Fig. 3(c) is the further development of the string inverter, where several strings are interfaced with their own dc–dc converter to a common dc–ac inverter [7], [28]. This is beneficial, compared with the centralized system, since every string can be controlled individually. Thus, the operator may start his/her own PV power plant with a few modules. Further enlargements are easily achieved since a new string with dc–dc converter can be plugged into the existing platform. A flexible design with high efficiency is hereby achieved.

Finally, the ac cell inverter system is the case where one large PV cell is connected to a dc–ac inverter [11]–[13]. The main challenge for the designers is to develop an inverter that can amplify the very low voltage, 0.5 $\sim$ 1.0 V and 100 W per square meter, up to an appropriate level for the grid, and at the same time reach a high efficiency. For the same reason, entirely new converter concepts are required.

IV. Classifications of Inverter Topologies

Next follows a classification of different inverter technologies. The topologies are categorized on the basis of number of power processing stages, location of power decoupling capacitors, if they employ transformers or not, and types of grid interface.

A. Number of Power Processing Stages

The number of power processing stages, in cascade, is the first grouping here. Fig. 4 shows three cases of single- and multiple-stage inverters.

The inverter of Fig. 4(a) is a single-stage inverter, which must handle all tasks itself, i.e., MPPT, grid current control and, perhaps, voltage amplification. This is the typical configuration for a centralized inverter, with all the drawbacks associated with it. The inverter must be designed to handle a peak power of twice the nominal power, according to (1).

Fig. 4(b) depicts a dual-stage inverter. The dc–dc converter is now performing the MPPT (and perhaps voltage amplification). Dependent on the control of the dc–ac inverter, the output from the dc–dc converters is either a pure dc voltage (and the dc–dc converter is only designed to handle the nominal power), or the output current of the dc–dc converter is modulated to follow a rectified sine wave (the dc–dc converter should now handle a peak power of twice the nominal power). The dc–ac inverter is in the former solution controlling the grid current by means of pulsewidth modulation (PWM) or bang-bang operation. In the latter, the dc–ac inverter is switching at line frequency, "unfolding" the rectified current to a full-wave sine, and the dc–dc converter takes care of the current control. A high efficiency can be reached for the latter solution if the nominal power is low. On the other hand, it is advisable to operate the grid-connected inverter in PWM mode if the nominal power is high.

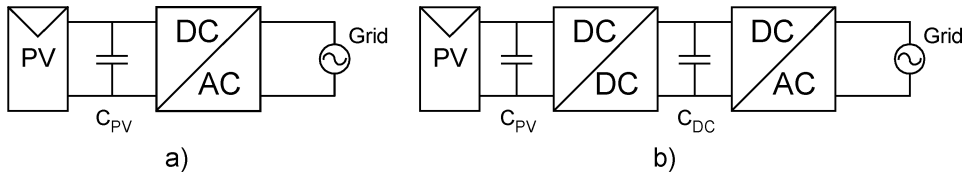

Fig. 5. Different locations for the power decoupling capacitor. (a) Capacitor is placed in parallel with the PV modules, in the case of a single-stage inverter. (b) Capacitor is either placed in parallel with the PV modules or in the dc link, in the case of a multi-stage inverter.

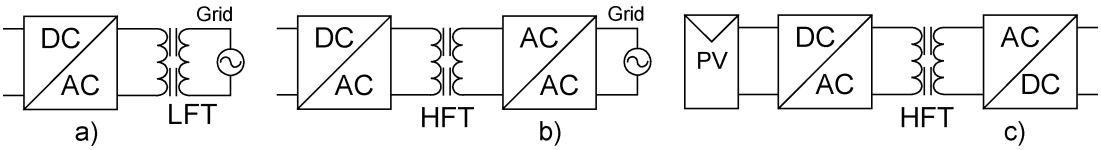

Fig. 6. Examples of transformer-included inverter solutions. (a) Line-frequency transformer (LFT) is placed between the grid and the inverter (solves problems with injection of dc currents into the grid). (b) High-frequency transformer (HFT) is embedded in an HF-link grid-connected ac/ac inverter. (c) HFT is embedded in a dc-link PV-module-connected dc–dc converter.

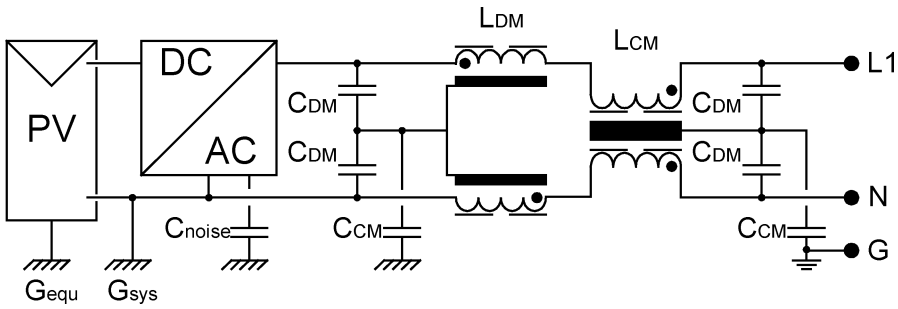

Fig. 7. Transformerless high-input-voltage PV inverter with single-phase common-mode (CM) and differential mode (DM) EMI filters.

Finally, Fig. 4(c) is the solution for the multi-string inverter. The only task for each dc–dc converter is MPPT and perhaps voltage amplification. The dc–dc converters are connected to the dc link of a common dc–ac inverter, which takes care of the grid current control. This is beneficial since better control of each PV module/string is achieved and that common dc–ac inverter may be based on standard VSD technology.

B. Power Decoupling

Power decoupling is normally achieved by means of an electrolytic capacitor. As stated earlier, this component is the main limiting factor of the lifetime. Thus, it should be kept as small as possible and preferably substituted with film capacitors. The capacitor is either placed in parallel with the PV modules or in the dc link between the inverter stages; this is illustrated in Fig. 5.

The size of the decoupling capacitor can be expressed as

$$C = \frac{P_{\mathrm{PV}}}{2 \cdot \omega_{\mathrm{grid}} \cdot U_C \cdot \hat{u}_C} \tag{9}$$

where P_{PV} is the nominal power of the PV modules, U_C is the mean voltage across the capacitor, and $\hat{u}_C$ is the amplitude of the ripple. Equation (9) is based on the fact that the current from the PV modules is a pure dc, and that the current drawn from the grid-connected inverter follows a $\sin^2(\omega_{\mathrm{grid}} \cdot t)$ waveform, assuming that U_C is constant. If the result from (2) ($U_{\mathrm{MPP}} = 35$ V, $\hat{u} = 3.0$ V, $P_{\mathrm{MPP}} = 160$ W) is used in (9), a capacitor of 2.4 mF is required in parallel with the PV module. On the other hand, if the capacitor is placed in the dc link, it becomes sufficient to use 33 μF at 380 V with a ripple amplitude of 20 V for the same PV module.

C. Transformers and Types of Interconnections

As stated earlier, some inverters use a transformer embedded in a high-frequency dc–dc converter or dc–ac inverter, others use a line-frequency transformer toward the grid and, finally, some inverters do not include a transformer at all (see Fig. 6). The line-frequency transformer is regarded as a poor component due to increased size, weight, and price.

Modern inverters tend to use a high-frequency transformer. This results in entirely new designs, such as the printed circuit board (PCB) integrated magnetic components [36].

The transformer is a paradox within PV inverters. As stated previously, system grounding of the PV modules is not required as long as the maximum output voltage is below 50 V. On the other hand, it is hard to achieve high-efficiency voltage amplification without a transformer, when the input voltage is in the range from 23 to 45 V. Third, the transformer is superfluous when the input voltage becomes sufficiently high. A normal full-bridge inverter cannot be used as grid interface, when both the input and the output of the inverter are be grounded.In addition, the large area of PV modules includes a capacitance of 0.1 nF $\sim$ 10 nF per module to ground [25]. This can also cause severe oscillations between the PV modules and (stray) inductances in the circuit.

Only a few high-input-voltage transformerless topologies that can be grounded both at the input and at the output are yet known; one configuration is illustrated in Fig. 7.

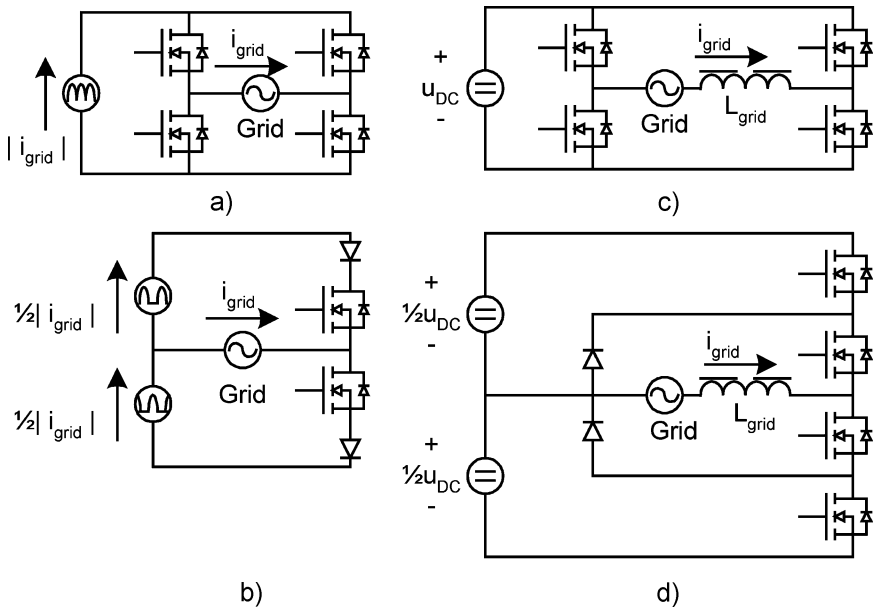

Fig. 8. Grid-connected inverter stages. (a), (b) Line-commutated CSI switching at twice the line frequency. (c), (d) Self-commutated voltage-source inverter (VSI) switching with high frequency in PWM or bang-bang mode.

D. Types of Grid Interfaces

Only inverters operating in current-source mode are included in the classification, since one of the aims of the PV inverter is to inject a sinusoidal current into the grid.

Fig. 8 shows four, out of many, possible grid-connected inverters. The topologies of Fig. 8(a) and (b) are line-frequency-commutated current-source inverters (CSIs). The current into the stage is already modulated/controlled to follow a rectified sinusoidal waveform and the task for the circuit is simply to re-create the sine wave and inject it into the grid. The circuits apply zero-voltage switching (ZVS) and zero-current switching (ZCS), thus, only conduction losses of the semiconductors remain.

Since the current is modulated by another stage, the other stage must be designed for a peak power of twice the nominal power, according to (1) and power decoupling must be achieved with a capacitor in parallel with the PV module(s). The converter feeding the circuit of Fig. 8(a) can be a push–pull with a single secondary transformer winding, and a flyback with two secondary windings for the circuit of Fig. 8(b).

The topology in Fig. 8(c) is a standard full-bridge three-level VSI, which can create a sinusoidal grid current by applying the positive/negative dc-link or zero voltage, to the grid plus grid inductor. The voltage across the grid and inductor is often pulsewidth modulated, but hysteresis (bang-bang) current control can also be applied. A variant of the topology in Fig. 8(c) is the half-bridge two-level VSI, which can only create two distinct voltages across and requires double dc-link voltage and double switching frequency in order to obtain the same performance as the full bridge.

The topology in Fig. 8(d), which is the half-bridge diode-clamped three-level VSI, is one of many different multilevel VSIs, which can create 3, 5, 7. . . distinct voltages across the grid and inductor. This is beneficial since the switching frequency of each transistor can be reduced and, in the mean time, good power quality is ensured.

The command signals for the transistors in the CSI and the reference for the grid-current waveform are mostly based on measured grid voltage or zero-crossing detection. This may result in severe problems with power quality and unnecessary fault situations. According to [8], the main reasons for these problems are the background (voltage) harmonics and poor design. The harmonics may initiate series resonance with the capacitors placed around in the grid (e.g., in refrigerators), due to positive feedback of the inverter current or a noisy signal from the zero-crossing detection. A solution for this problem is to use a phase-locked loop (PLL) for establishing a current waveform reference of high quality.

V. AC Modules

The ac Module is the combination of one PV module with a grid-connected inverter [see Fig. 3(d)]. According to the above discussion, the inverters should be of the dual-stage type with an embedded HF transformer. Reviews of ac module inverters are given in [25]–[35]. Next follow some classical solutions for the ac module inverters. The results from the literature survey are compiled in Table II.

The topology shown in Fig. 9 is a 100-W flyback-type inverter [37]. The circuit is made up around a single-transistor flyback converter, with a center-tapped transformer. The two outputs from the transformer are connected to the grid, one at a time, through two MOSFETs, two diodes, and a common filter circuit [37]. The flyback converter can, in this way, produce both a positive and a negative output current.

The next topology in Fig. 10 is a 105-W combined flyback and buck–boost inverter [38]. The need for a large decoupling capacitor is avoided by adding a buck–boost converter to the flyback converter. The leakage inductance included in the transformer results in a voltage spike across the transistor denoted

TABLE II
SUMMARY OF THE AC MODULE INVERTERS. FOR THE EFFICIENCY, M REFERS TO THE MAXIMUM EFFICIENCY, E TO THE EUROPEAN EFFICIENCY, AND N TO NOMINAL CONDITION EFFICIENCY

Fig. and ref.	9 [37]	10 [38]	11 [39]	12 [40]	13 [41]	14 [43], [44]	15 [36], [45]	16 [46]
Nominal power [W]	100	105	160	160	150	100	110	90
Grid voltage [V]	230	85	230	100	120	210	230	230
Input voltage [V]	48	35	28	-	44	30	30	24-40
Efficiency [%]	96M	-	82E, 87M	-	-	-	87N	91E, 93M
Power factor [ ]	0.955	-	-	-	-	-	-	0.99
THD [%]	-	<5	-	-	-	-	-	-

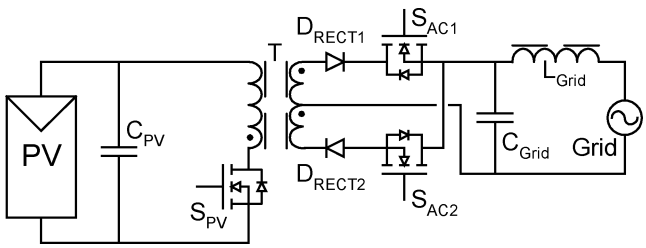

Fig. 9. 100-W single-transistor flyback-type HF-link inverter [37].

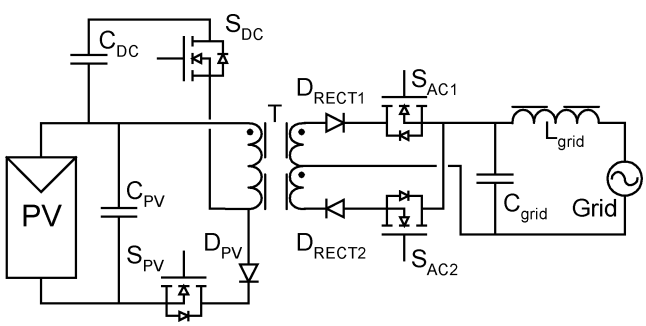

Fig. 10. Flyback-type inverter with high-power decoupling [38].

S_{DC} in Fig. 10, during turn-off. A dissipative *RCD* clamp would normally be used to remove the overvoltage; see the previous topology. However, the *RCD* clamp circuit interacts heavily with the buck–boost circuit, causing the inverter to malfunction. The solution is the modified Shimizu topology presented in the next section [39]. Finally, the energy-storing capacitor C_{DC} must carry the entire load current, which increases the demands for its current-ripple capabilities.

The inverter in Fig. 11 is an enhanced version of the previous topology, rated for 160 W. The main improvement within this inverter is the replacement of the single-transistor flyback converter with a two-transistor flyback converter, to overcome problems with overvoltage.

The topology in Fig. 12 is a 160-W buck–boost inverter [40]. Again, a small amount of energy is stored in the leakage inductance. This energy is now recovered by the body diodes of transistors S_{PV2} and S_{PV3}. On the other hand, the diode D_{PV} is blocking for the energy recovery, and no further information is given in [40] about the type of applied clamp circuit.

The topology in Fig. 13 is a 150-W flyback dc–dc converter together with a line-frequency dc–ac unfolding inverter [41]. In [42], the same topology is applied for a 100-W inverter, except that the grid filter is removed from the dc link to the grid side. The line-frequency dc–ac inverter is in both cases equipped with thyristors, which can be troublesome to turn on, since they require a current in their control terminal to turn on.

The inverter in Fig. 14 is a 100-W flyback dc–dc converter together with a PWM dc–ac inverter [43], [44]. The output stage is now made up of four transistors, which are switched at high frequency. The grid current is modulated by alternately connecting the positive or the negative dc-link voltage (the constant voltage across C_{DC}) to the inductor L_{grid} in $D \times T_{\mathrm{sw}}$ s, and zero voltage in $(1 - D) \times T_{\mathrm{sw}}$ (D is the duty cycle and T_{sw} is the switching period).

The inverter in Fig. 15 is based on a 110-W series-resonant dc–dc converter with an HF inverter toward the grid [36], and 250 W in [45]. The series-resonant converter is the first resonant converter visited here. The inverter toward the grid is modified in such a way that is cannot operate as a rectifier, seen from the grid side. Adding two additional diodes does this. The advantage of this solution is that no in-rush current flows when the inverter is attached to the grid for the first time.

The commercially available Mastervolt Soladin 120 inverter [46] is a "plug-and-play" inverter, based on the topology in Fig. 16. The nominal input power is 90 W at 20–40 V, but the opportunity to operate at peak 120 W exists. The Soladin 120 inverter is a dual-stage topology without inherent power decoupling. The capacitor in parallel with the PV module is, therefore, rather larger (2 × 1000 mF at 50 V), since it must work as an energy buffer. According to the work in Section II-B, this results in a small-signal amplitude in the range from 1.8 to 3.0 V, which corresponds to a PV utilization factor from 0.984 to 0.993 at full generation.

VI. STRING AND MULTI-STRING INVERTERS

The string and multi-string systems are the combination of one or several PV strings with a grid-connected inverter

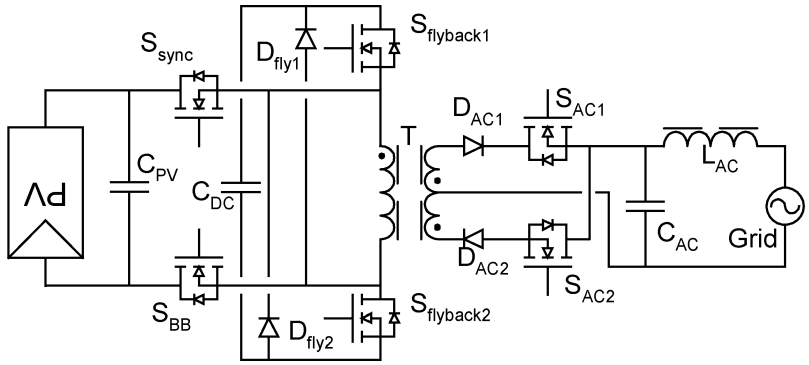

Fig. 11. Modified Shimizu inverter [39]. Note that the polarity of the PV module is reversed.

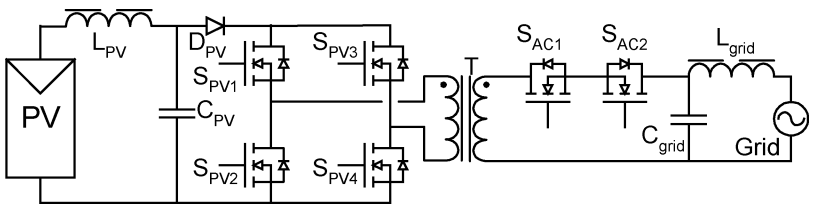

Fig. 12. Dual two-transistor flyback-type inverter [40].

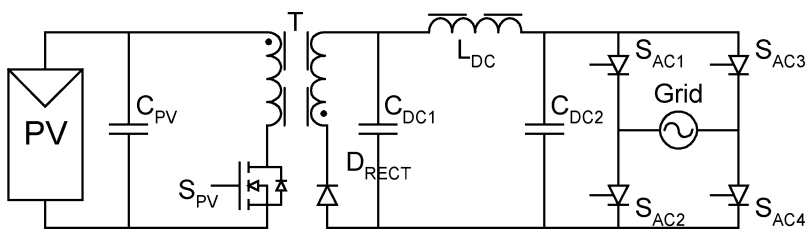

Fig. 13. Flyback dc–dc converter with unfolding dc–ac inverter [41].

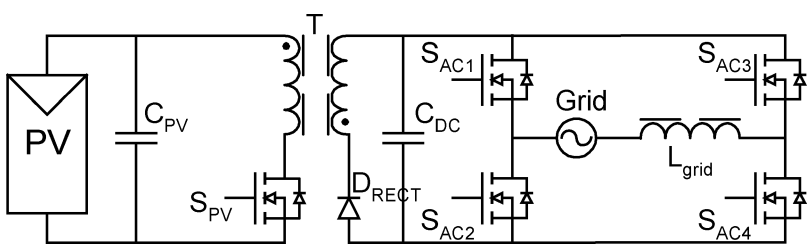

Fig. 14. Flyback dc–dc converter with PWM inverter [43], [44].

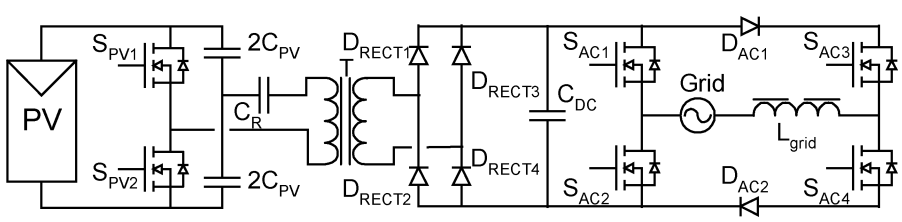

Fig. 15. Series-resonant dc–dc converter with bang-bang dc–ac inverter [36], [45].

[see Fig. 3(b) and (c). According to the above discussion, the inverters should be of the single- or dual-stage type with or without an embedded HF transformer. Next follow some classical solutions for the string and multi-string inverters.

The inverter in Fig. 17 is a transformerless half-bridge diode-clamped three-level inverter [25], [47]. Turning S_1 andS_2 on can create a positive output voltage, turningS_2 and S_3 on creates zero voltage, and finally, turning S_3 and S_4 on creates a negative voltage. Each of the two PV strings is connected to the ground/neutral of the grid, thus, the capacitive earth currents are reduced, and the inverter can easily fulfill the NEC 690 standard. The inverter can be further extended to five levels by adding more transistors, diodes, and PV strings. However, this requires that the outer strings (e.g., the strings placed at locations #0 and #4 in Fig. 17, not illustrated) must be carefully sized since they are loaded differently than strings #1 and #2. Another serious

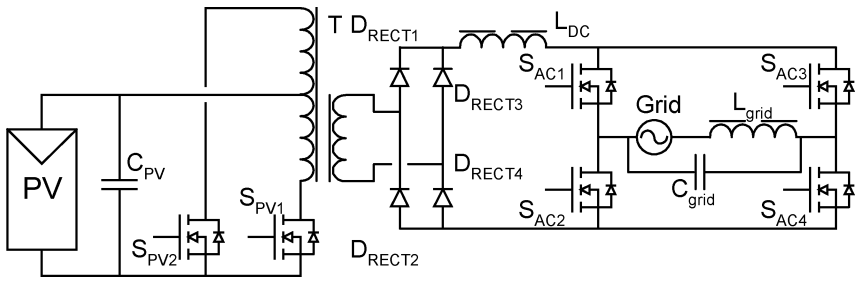

Fig. 16. Soladin 120 commercial inverter [14].

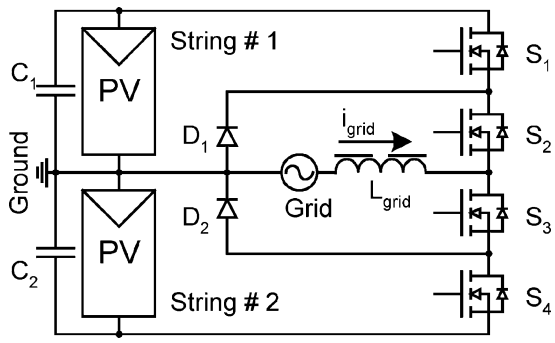

Fig. 17. Grid-connected system with half-bridge diode-clamped three-level inverter (HBDC) [25], [47].

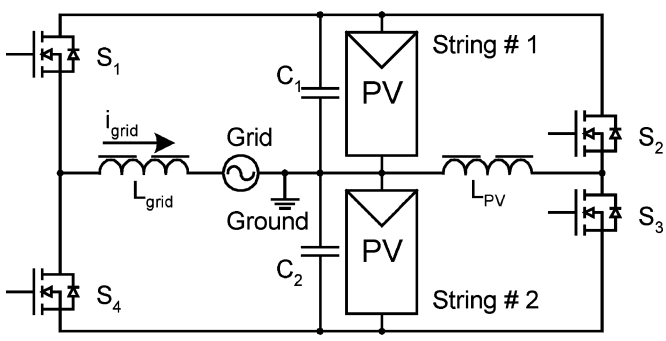

Fig. 18. Utility interactive photovoltaic inverter with GCC [48], [49].

drawback is that string #1 is only loaded during positive grid voltage, and vise versa for string #2. This requires the decoupling capacitors to be enlarged with a factor of approximately π, compared to Section IV-B. This is not an advantage for the cost or the lifetime.

The inverter in Fig. 18 is a two-level VSI, interfacing two PV strings [48], [49]. This inverter can only produce a two-level output voltage, thus, the switching frequency must be double the previous one in order to obtain the same size of the grid inductor. The main difference between this and the former topology is the generation control circuit (GCC), made by transistors S_2 and S_3 and inductor L_{PV}, which can load each PV string independently. Actually, one of the PV strings can even be removed and sinusoidal current can still be injected into the grid. The GCC is an advantage since an individual MPPT can be applied to each string. Further enlargement is easily achieved by adding another PV string plus a transistor, a capacitor, and an inductor. The drawback of this topology and the topology in Fig. 17 is their buck characteristic, for which reason the minimum input voltage always must be larger than the maximum grid voltage. For example, the maximum grid voltage is equal to $230 \cdot \sqrt{2} \cdot 1.1 \approx 360$ V, and the minimum voltage across a PV module is 23 V $-$ 3 V (MPP voltage minus the 100-Hz ripple across the PV strings). Hence, two strings, each of minimum 18 modules, are required for the former topology and two strings of minimum nine modules for the latter topology.

The commercially available inverter (SMA Sunny Boy 5000TL [33], [50]) in Fig. 19 is designed for three PV strings, each of 2200 W at 125 $\sim$ 750 V, and each with their own MPPT. The circuits interfacing the PV strings are standard boost converters, which is beneficial since the HF current ripple at the input terminals of the converters is easily filtered by a film capacitor. The grid-connected dc–ac inverter is a two-level VSI. When this is pointed out, it becomes obvious that the PV strings cannot be system grounded, thus, this inverter is not allowed in the U.S. due to the NEC 690 standard.

Finally, the original equipment manufacturer (OEM) inverter (PowerLynx Powerlink PV 4.5 kW [51], [52]) in Fig. 20 is also designed for three PV strings, each with an input range from 200 to 500 V and 1500 W. The dc–dc converters are based on current-source full-bridge inverters with embedded HF transformer and rectifier. The PV strings are easily system grounded and no problem with the NEC 690 standard exists, since this inverter includes galvanic isolation between the PV string and the grid. Once again, the current-source input stage is beneficial since it reduces the requirement for the filter capacitor in parallel with the PV strings. Furthermore, the diodes included in the rectifiers are current commutated which involves low reverse recovery of the diodes and low voltage stress. The grid-connected dc–ac inverter is a three-level VSI.

VII. Discussion

A. Methods

The presented ac module inverters have all been evaluated in [14] for component ratings, relative cost, lifetime, and European efficiency. The results are shown in Table III.

The ratings of the semiconductors are based on the average or rms currents and the peak voltages they have to withstand, together with a de-rating factor of 0.23 (composed of a 0.75 de-rate factor for the peak voltage and a 0.30 de-rate factor for the rms value of the current), e.g., the PV side transistors in the inverter of Fig. 16 must withstand 90 V peak and 7.6-A rms, thus, their VA ratings are computed as 3.0 kVA each. The ratings

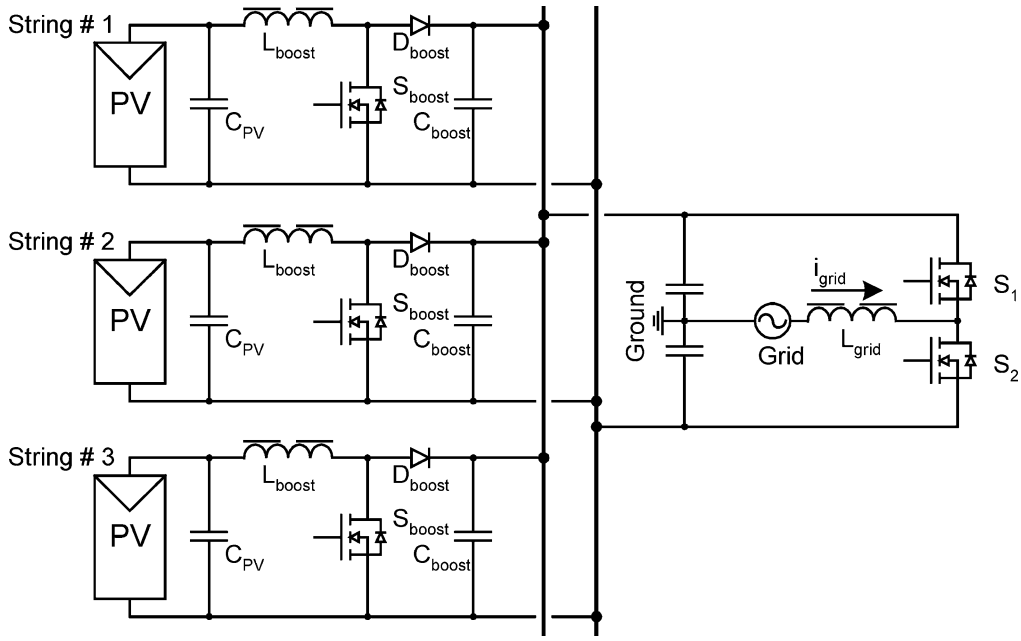

Fig. 19. Topology of the power electronics of the multi-string inverter in [33] and [50]: Sunny Boy 5000TL. Maximum power per string equals 2200 W at 125 $\sim$ 750 V.

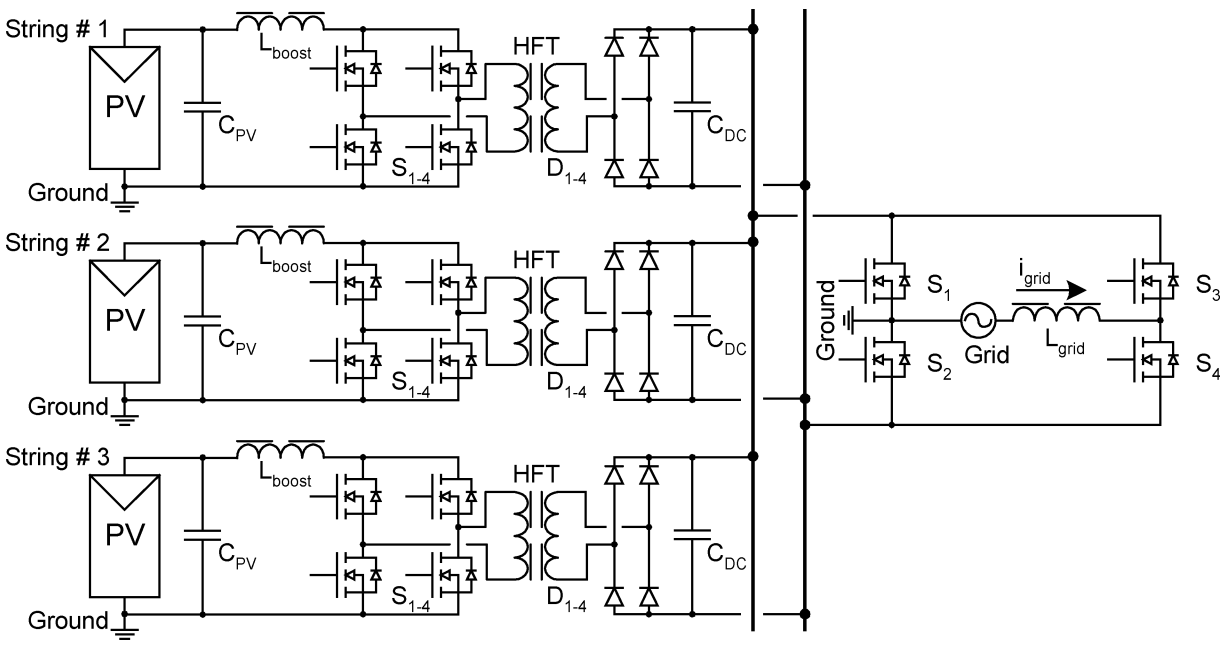

Fig. 20. Topology of the power electronics of the three-string inverter in [21]–[23], [51], and [52]. Maximum power per string equals 1500 W at 200 $\sim$ 500 V.

for the transformers are based on the geometrical core constant approach in [24]

$$K_{g,\mathrm{Fe}} = \frac{\rho \cdot \lambda^2 \cdot I_{\mathrm{tot}}^2 \cdot (K_{\mathrm{Fe}} \cdot f_{\mathrm{sw}}^{\alpha})^{\left(\frac{2}{\beta}\right)}}{4 \cdot K_U \cdot P_{\mathrm{tot}}^{\left(\frac{(\beta+2)}{\beta}\right)}} \cdot 10^8 \ \mathrm{cm}^x \tag{10}$$

where ρ is the winding resistivity, λ is the applied volt-seconds on the primary turns, I_{tot} is the total winding current, f_{sw} is the switching frequency, K_U is the copper fill factor, P_{tot} is the total power loss in the transformer, and K_{Fe}, α, and β are some coefficients describing the core loss as functions of peak flux density and frequency. The total power loss in the core is limited to a value that guarantees a maximum temperature difference between the ambient and core surface of no more then 40 °C.

The relative cost is computed on the basis of the calculated ratings, a component survey at different vendors, and linear regression analysis. The following relationship is used to determine the relative cost:

$$EURO = 0.458 \cdot E + 0.738 \text{ for electrolytic capacitors} \tag{11}$$

$$EURO = 227.3 \cdot K_{g,\mathrm{Fe}} + 1.746 \text{ for magnetics} \tag{12}$$

$$EURO = 0.263 \cdot \mathrm{kVA} + 0.511 \text{ for PV-side MOSFETs} \tag{13}$$

TABLE III
EVALUATION OF THE SEVEN INVERTER TOPOLOGIES FOR THE AC MODULE

Fig. No.	Decoupling capacitor	Lifetime	Grid interface	European efficiency [%]	Cost [Euro]	Component ratings (besides EMI filter)	
-	-	-	-	-	-	T [cm^x]	S+D [kVA]
9	2.2 mF @ 45 V	Medium	2 transistor CSI	91.4	19.6	0.0115	12.3
11	68 µF @ 160 V	Short	2 transistor CSI	69.7	27.6	0.0173	36.5
12	2.2 mF @ 45 V	Medium	2 transistor CSI	92.0	22.6	0.0115	13.7
13	2.2 mF @ 45 V	Medium	4 transistor CSI	92.4	20.7	0.0115	16.0
14	33 µF @ 400 V	Long	4 transistor VSI	90.3	19.4	0.0081	14.0
15	33 µF @ 400 V	Long	4 transistor VSI	90.5	25.3	0.0041	13.3
16	2.2 mF @ 45 V	Medium	4 transistor CSI	95.4	21.1	0.0115	18.5

T – Transformer, S+D – Semiconductors.

TABLE IV
EVALUATION OF THE FOUR STRING AND MULTI-STRING INVERTER TOPOLOGIES. THE POWER DECOUPLING CAPACITORS ARE COMPUTED WITH (9). THE NUMBER OF PV MODULES PER STRING IS COMPUTED ON THE BASIS OF RATED POWER AND VOLTAGE RANGE

Fig. No.	Number of stages / strings	Power decoupling	Grid interface	Dual grounding and isolation	Min. input voltage	Nominal AC power	Reported efficiency	THD	Number of components (besides EMI filter)			
-	-	-	-	-	-	-	-	-	T	L/F/E	S/D	PV
17	1 / 2, 4, 6...	2× (640 µF at 810 V)	Three-level	Yes / No	2 × 360V	5.8 kW	-	-	0	1/2/2	4/2	2× 18
18	2 / (1), 2, (3), 4 ...	2× (410 µF at 405 V)	Two-level	Yes / No	360 V	2.9 kW	-	-	0	2/2/2	4/0	2× 9
19	2 / 1, 2, 3	2× (1200 µF at 375 V)	Two-level	No / No	150 V	4.6 kW	95.0%	<4%	0	4/3/2	5/3	3× 13
20	2 / 1, 2, 3	3× (310 µF at 400 V)	Three-level	Yes / Yes	200 V	4.5 kW	94.5%	5%	3× HF	4/3/3	16/12	3× 9

T – Transformer, L – Inductor, F – Film Capacitor, E – Electrolytic Capacitor, S – Transistor, D – Diode, PV – Photovoltaic Modules.

$$EURO = 0.570 \cdot \text{kVA} + 0.184 \text{ for grid-side MOSFETs} \tag{14}$$

$$EURO = 0.134 \cdot \text{kVA} + 0.090 \text{ for rectifier diodes} \tag{15}$$

where E is the energy stored in the capacitor, i.e., $1/2 \cdot C \cdot U_C^2$, and kVA is the computed ratings for the semiconductors.

The lifetime is evaluated by the size of the de-coupling capacitors, and the amount of current they have to carry. A high current involves high power loss in the capacitors, which results in hot spots inside the capacitors, and an increased temperature is the main factor of the lifetime.

The efficiency for each inverter has been computed at six different operating points, based on "average" components from the component survey. According to the definition of the European efficiency, the individual efficiencies are weighted and summed up according to

$$\eta_{EU} = 0.03 \cdot \eta_{5\%} + 0.06 \cdot \eta_{10\%} + 0.13 \cdot \eta_{20\%} + 0.10 \cdot \eta_{30\%} + 0.48 \cdot \eta_{50\%} + 0.20 \cdot \eta_{100\%} \tag{16}$$

where the index value is equal to percent of rated power [32]. This is done in order to make a fair comparison of the inverters, under partial load conditions.

B. AC Module Inverters

Dual-stage CSIs like the circuits in Fig. 8(a) and (b) suffer from a large electrolytic decoupling capacitor, whereas decoupling for the VSI can be achieved with a small electrolytic capacitor. This is beneficial when lifetime is the issue, since, as already stated, the electrolytic capacitor is the main limiting single component within the inverters.

Only two circuits are different from the others when examining the European efficiency; these are the inverters in Figs. 11 and 16. The inverter in Fig. 11 has a low efficiency, which is caused by the high voltage ratings for the semiconductors on the PV side, and in the mean time, high current also flows in the circuit. The push–pull inverter in Fig. 16 has a higher efficiency than the other inverters. This is mainly due to a low conduction loss in the PV-side converter, where only two transistors are carrying the current. On the other hand, the voltage stress for the two transistors is double that of the other inverters (except the one in Fig. 11). This is also seen in the ratings of the semiconductors for this inverter, which are higher than the others. If one should select an inverter topology based on this comparison, the push–pull inverter in Fig. 16 would be a preferable choice, since it offers high efficiency and relatively low price, but attention should be paid to the decoupling capacitor, which is the weakest point.

C. String and Multi-String Inverters

The string and multi-string inverters presented in this review represent the latest development within this area. The inverters are summarized in Table IV.

The dual-grounded multilevel HBDC inverters can be a good solution, but attention should be paid to the decoupling capacitors, which in the case of the inverter in Fig. 17 must be rather large since they are only loaded in half of the grid period. A solution could be to include some kind of balancing circuit, like the balancing GCC in Fig. 18.

Two of the reviewed topologies, (see Figs. 18 and 19) use bipolar PWM switching toward the grid. This is beneficial for the GCC inverter in Fig. 18, but not for the topology in Fig. 19 due to the requirement for a high dc-link voltage and two decoupling capacitors in series to create a midpoint. Besides this, the inverter in Fig. 19 cannot be system grounded which is a requirement from the NEC 690 standard, but common-mode electrical noise at the terminals of the PV module can also generate large ground currents, due to the capacitances from the PV modules to ground.

The last topology visited here is based on current-fed full-bridge dc–dc converters with embedded HF transformers, for each PV string. This requires more components than the three previous inverters, but their ratings are lower and the benefits of mass production could be easily achieved. Both commercially available inverters show good efficiency and grid performance.

VIII. Conclusion

This review has covered some of the standards that inverters for PV and grid applications must fulfill, which focus on power quality, injection of dc currents into the grid, detection of islanding operation, and system grounding. The demands stated by the PV modules have also been reviewed; in particular, the role of power decoupling between the modules and the grid has been investigated. An important result is that the amplitude of the ripple across a PV module should not exceed 3.0 V in order to have a utilization efficiency of 98% at full generation. Finally, the basic demands defined by the operator have also been addressed, such as low cost, high efficiency, and long lifetime.

The next part of the review was a historical summary of the solutions used in the past, where large areas of PV modules were connected to the grid by means of centralized inverters. This included many shortcomings for which reason the string inverters emerged. A natural development was to add more strings, each with an individual dc–dc converter and MPPT, to the common dc–ac inverter, thus, the multi-string inverters were brought to light. This is believed to be one of the solutions for the future. Another trend seen in this field is the development of the ac module, where each PV module is interfaced to the grid with its own dc–ac inverter.

The historical review was followed with a classification of the inverters: number of power processing stages, type of power decoupling between the PV module and the grid, transformers and types of interconnections between the stage, and types of grid interfaces. The conclusions from the classifications are as follows.

1) Large centralized single-stage inverters should be avoided, except if the input voltage is sufficiently high to avoid further amplification. The dual-stage inverter is the solution for ac modules and ac cells, since they require voltage amplification. Last, if several strings are to be connected to the grid, the multi-sting concept seems to be the obvious choice.
2) Nothing is gained by moving the decoupling capacitor from the input of the inverter to the dc link, when PV modules are connected in series to reach a high voltage for the inverter. On the other hand, in the case of the ac module and the ac cell, the preferable location for the capacitor is in the dc link where the voltage is high and a large fluctuation can be allowed without compromising the utilization factor. Electrolytic capacitors should be replaced with film capacitors in order to increase the reliability, but this also involves a higher price, especially for high-power inverters, where a large capacitance is required. On the other hand, a high reliability can be a major sales parameter.
3) HFTs should be applied for voltage amplification in the ac module and ac cell concepts. It is also beneficial to include an HFT in larger systems in order to avoid resonance between the PV modules and inductances in the current main paths. The resonance can, however, also be mitigated with inverter topologies that support grounding on both input and the output terminals. The dual grounding scheme is also a requirement in the U.S. for PV open-circuit voltages larger then 50 V, but not in Europe and Japan.
4) Line-frequency CSIs are suitable for low power, e.g., for ac module applications. On the other hand, a high-frequency VSI is also suitable for both low- and high-power systems, like the ac module, the string, and the multi-string inverters.

The rules to judge the examined inverters were then established, and seven ac module inverters and four multi-string inverters were reviewed. This concluded in a discussion of each of the topologies. Based on work in [14] the most suitable inverter for a 160-W ac mmodule is recognized as being the one in Fig. 16. The work in [14] does not deal with inverters for string and multi-string PV systems, but based on the review given here, the best candidates seem to be the inverters of Figs. 18 and 20.

References

Standards and Texts Articles

[1] J. P. Benner and L. Kazmerski, "Photovoltaics gaining greater visibility," *IEEE Spectr.*, vol. 29, no. 9, pp. 34–42, Sep. 1999.

[2] (2003) Trends in Photovoltaic Applications. Survey Report of Selected IEA Countries Between 1992 and 2002. International Energy Agency Photovoltaic Power Systems, IEA PVPS T1-12:2003. [Online]. Available: www.iea-pvps.org

[3] *Characteristics of the Utility Interface for Photovoltaic (PV) Systems*, IEC 61727 CDV (Committee Draft for Vote), 2002.

[4] *Limits for Harmonic Current Emission (Equipment Input Current <16 A per Phase)*, EN 61000-3-2, 1995.

[5] *IEEE Standard for Interconnecting Distributed Resources With Electric Power Systems*, IEEE Std. 1547, 2003.

[6] *2002 National Electrical Code*, National Fire Protection Association, Inc., Quincy, MA, 2002.

[7] B. Verhoeven *et al.*. (1998) Utility Aspects of Grid Connected Photovoltaic Power Systems. International Energy Agency Photovoltaic Power Systems, IEA PVPS T5-01: 1998. [Online]. Available: www.iea-pvps.org

[8] J. H. R. Enslin and P. J. M. Heskes, "Harmonic interaction between a large number of distributed power inverters and the distribution network," in *Proc. IEEE PESC'03*, vol. 4, 2003, pp. 1742–1747.

[9] O. Willumsen, "Connection of solar systems," Danish Electricity Supply—Research and Development (DEFU), Copenhagen, Denmark, Tech. Rep. 501, 2003.

[10] E. Bezzel, H. Lauritzen, and S. Wedel. (2004) The photo electro chemical solar cell. PEC Solar Cell Project, Danish Technological Institute. [Online]. Available: www.solarcell.dk

[11] H. Wilk, D. Ruoss, and P. Toggweiler. (2002) Innovative electrical concepts. International Energy Agency Photovoltaic Power Systems, IEA PVPS 7-07:2002. [Online]. Available: www.iea-pvps.org

[12] M. Wuest, P. Toggweiler, and J. Riatsch, "Single cell converter system (SCCS)," in *Proc. 1st IEEE WCPEC*, vol. 1, 1994, pp. 813–815.

[13] J. Riatsch, H. Stemmler, and R. Schmidt, "Single cell module integrated converter system for photovoltaic energy generation," in *Proc. EPE'97*, vol. 1, Trondheim, Norway, 1997, pp. 71–77.

[14] S. B. Kjaer, "Design and control of an inverter for photovoltaic applications," Ph.D. dissertation, Inst. Energy Technol., Aalborg University, Aalborg East, Denmark, 2004/2005.

[15] S. Poulsen, "Global and Danish reference year irradiation," Danish Technological Inst., Taastrup, Denmark, 2002.

[16] H. Oldenkamp, I. J. de Jong, C. W. A. Baltus, S. A. M. Verhoeven, and S. Elstgeest, "Reliability and accelerated life tests of the AC module mounted OKE4 inverter," in *Proc. IEEE Photovoltaic Specialists Conf.*, 1996, pp. 1339–1342.

[17] P. Rooij, M. Real, U. Moschella, T. Sample, and M. Kardolus. (2001) Advanced Reliability Improvements of AC-Modules (ARIA), ECN-C-01-093. Netherlands Energy Research Foundations (ECN). [Online]. Available: www.ecn.nl

[18] C. W. G. Verhoeve, C. F. A. Frumau, E. de Held, and W. C. Sinke. (1997) Reliability testing of ac-module inverters. *Conf. Rec. 14th European Photovoltaic Solar Energy Conference*. [Online]. Available: www.ecn.nl

[19] R. H. Bonn, "Developing a 'next generation' PV inverter," in *Conf. Rec. 29th IEEE Photovoltaic Specialists Conf.*, 2002, pp. 1352–1355.

[20] (2001, Feb.) Electrolytic Capacitors Application Guide, EVOX RIFA, ID 830G. [Online]. Available: www.evox-rifa.com

[21] R. Teodorescu, F. Blaabjerg, U. Borup, and M. Liserre, "A new control structure for grid-connected LCL PV inverters with zero steady-state error and selective harmonic compensation," in *Proc. IEEE APEC'04*, vol. 1, 2004, pp. 580–586.

[22] L. Asiminoaei, R. Teodorescu, F. Blaabjerg, and U. Borup, "A new method of on-line grid impedance estimation for PV inverter," in *Proc. IEEE APEC'04*, vol. 3, 2004, pp. 1527–1533.

[23] A. V. Timbus, R. Teodorescu, F. Blaabjerg, and U. Borup, "Online grid measurement and ENS detection for PV inverter running on highly inductive grid," *IEEE Power Electron. Lett.*, vol. 2, no. 3, pp. 77–82, Sep. 2004.

[24] R. W. Erickson and D. Maksimovic, *Fundamentals of Power Electronics*, 2nd ed. Norwell, MA: Kluwer, 2001.

Review Articles

[25] M. Calais, J. Myrzik, T. Spooner, and V. G. Agelidis, "Inverters for single-phase grid connected photovoltaic systems—An overview," in *Proc. IEEE PESC'02*, vol. 2, 2002, pp. 1995–2000.

[26] Y. Xue, L. Chang, S. B. Kjaer, J. Bordonau, and T. Shimizu, "Topologies of single-phase inverters for small distributed power generators: an overview," *IEEE Trans. Power Electron.*, vol. 19, no. 5, pp. 1305–1314, Sep. 2004.

[27] F. Blaabjerg, Z. Chen, and S. B. Kjaer, "Power electronics as efficient interface in dispersed power generation systems," *IEEE Trans. Power Electron.*, vol. 19, no. 5, pp. 1184–1194, Sep. 2004.

[28] M. Meinhardt and G. Cramer, "Past, present and future of grid connected photovoltaic- and hybrid-power-systems," in *Proc. IEEE-PES Summer Meeting*, vol. 2, 2000, pp. 1283–1288.

[29] M. Calais and V. G. Agelidis, "Multilevel converters for single-phase grid connected photovoltaic systems—an overview," in *Proc. IEEE ISIE'98*, vol. 1, 1998, pp. 224–229.

[30] J. M. A. Myrzik and M. Calais, "String and module integrated inverters for single-phase grid connected photovoltaic systems—A review," in *Proc. IEEE Bologna PowerTech Conf.*, vol. 2, 2003, pp. 430–437.

[31] S. B. Kjaer, J. K. Pedersen, and F. Blaabjerg, "Power inverter topologies for photovoltaic modules—A review," in *Conf. Rec. IEEE-IAS Annu. Meeting*, vol. 2, 2002, pp. 782–788.

[32] H. Haeberlin, "Evolution of inverters for grid connected PV-systems from 1989 to 2000," in *Proc. 17th Eur. Photovoltaic Solar Energy Conf.*, Munich, Germany, Oct. 22–26, 2001, pp. 426–430.

[33] M. Meinhardt and G. Cramer, "Multi-string-converter: The next step in evolution of string-converter technology," in *Proc. 9th Eur. Power Electronics and Applications Conf.*, 2001, CD-ROM.

[34] H. Oldenkamp and I. J. de Jong, "AC modules: past, present and future," in *Proc. Workshop Installing the Solar Solution*, Hatfield, U.K., 1998.

[35] B. Lindgren, "Topology for decentralised solar energy inverters with a low voltage ac-bus," in *Proc. EPE'99*, 1999, CD-ROM.

AC Modules

[36] M. Meinhardt, T. O'Donnell, H. Schneider, J. Flannery, C. O. Mathuna, P. Zacharias, and T. Krieger, "Miniaturised 'low profile' module integrated converter for photovoltaic applications with integrated magnetic components," in *Proc. IEEE APEC'99*, vol. 1, 1999, pp. 305–311.

[37] N. P. Papanikolaou, E. C. Tatakis, A. Critsis, and D. Klimis, "Simplified high frequency converter in decentralized grid-connected PV systems: a novel low-cost solution," in *Proc. EPE'03*, 2003, CD-ROM.

[38] T. Shimizu, K. Wada, and N. Nakamura, "A flyback-type single phase utility interactive inverter with low-frequency ripple current reduction on the DC input for an AC photovoltaic module system," in *Proc. IEEE PESC'02*, vol. 3, 2002, pp. 1483–1488.

[39] S. B. Kjaer and F. Blaabjerg, "Design optimization of a single phase inverter for photovoltaic applications," in *Proc. IEEE PESC'03*, vol. 3, 2003, pp. 1183–1190.

[40] M. Nagao and K. Harada, "Power flow of photovoltaic system using buck-boost PWM power inverter," in *Proc. PEDS'97*, vol. 1, 1997, pp. 144–149.

[41] S. Mekhilef, N. A. Rahim, and A. M. Omar, "A new solar energy conversion scheme implemented using grid-tied single phase inverter," in *Proc. IEEE TENCON'00*, vol. 3, 2000, pp. 524–527.

[42] E. Achille, T. Martiré, C. Glaize, and C. Joubert, "Optimized DC-AC boost converters for modular photovoltaic grid-connected generators," in *Proc. IEEE ISIE'04*, 2004, pp. 1005–1010.

[43] D. C. Martins and R. Demonti, "Grid connected PV system using two energy processing stages," in *Conf. Rec. 29th IEEE Photovoltaic Specialists Conf.*, 2002, pp. 1649–1652.

[44] ——, "Photovoltaic energy processing for utility connected system," in *Proc. IEEE IECON'01*, vol. 2, 2001, pp. 1292–1296.

[45] A. Lohner, T. Meyer, and A. Nagel, "A new panel-integratable inverter concept for grid-connected photovoltaic systems," in *Proc. IEEE ISIE'96*, vol. 2, 1996, pp. 827–831.

[46] (2001, Oct.) Soladin 120. Mastervolt. [Online]. Available: www.mastervolt.com/sunmaster

String and Multi-String Inverters

[47] M. Meinhardt and P. Mutschler, "Inverters without transformer in grid connected photovoltaic applications," in *Proc. EPE'95*, vol. 3, 1995, pp. 86–91.

[48] T. Shimizu, M. Hirakata, T. Kamezawa, and H. Watanabe, "Generation control circuit for photovoltaic modules," *IEEE Trans. Power Electron.*, vol. 16, no. 3, pp. 293–300, May 2001.

[49] T. Shimizu, O. Hashimoto, and G. Kimura, "A novel high-performance utility-interactive photovoltaic inverter system," *IEEE Trans. Power Electron.*, vol. 18, no. 2, pp. 704–711, Mar. 2003.

[50] (2005, Jan.) Sunny Boy 5000TL Multi-String—Operating Instructions, SMA. [Online]. Available: www.sma.de

[51] C. Dorofte, "Comparative analysis of four dc/dc converters for photovoltaic grid interconnection," Aalborg Univ./Powerlynx A/S, Aalborg East, Denmark, Tech. Rep., 2001.

[52] ——, "Design of a dc/dc converter for photovoltaic grid interconnection," Aalborg Univ./Powerlynx A/S, Aalborg East, Denmark, Tech. Rep., 2001.

Soeren Baekhoej Kjaer (S'98-AM'00-M'04) received the M.Sc. and Ph.D. degrees in electrical engineering from Institute of Energy Technology, Aalborg University, Aalborg East, Denmark, in 2000 and 2005, respectively.

He is currently with PowerLynx A/S, Sønderborg, Denmark, where he works in the field of photovoltaic power. He was with the Section of Power Electronics and Drives, Aalborg University, from 2000 to 2004, where he was a Research Assistant and Laboratory Assistant. He also taught courses on photovoltaic systems for terrestrial and space applications (power system for the AAU student satellite: AAU CubeSat). His main interests are switching inverters, including power quality and control and optimized design for fuel-cell and, in particular, photovoltaic applications.

Mr. Kjaer is a Member of the Society of Danish Engineers (M.IDA).

John K. Pedersen (M'91–SM'00) was born in Holstebro, Denmark, in 959. He received the B.Sc.E.E. degree from Aalborg University, Aalborg East, Denmark.

He was with the Institute of Energy Technology, Aalborg University, as a Teaching Assistant from 1983 to 1984, and as an Assistant Professor from 1984 to 1989. He has been an Associate Professor since 1989. He is also the Head of the Institute of Energy Technology. His research areas are power electronics, power converters, and electrical drive systems, including modeling, simulation, and design with a focus on optimized efficiency.

Mr. Pedersen received the 1992 Angelos Award for his contribution to the control of induction machines. In 1998, he received an IEEE TRANSACTIONS ON POWEr ELECTRONICS Prize Paper Award for the best paper published in 1997.

Frede Blaabjerg (S'86–M'88–SM'97–F'03) was born in Erslev, Denmark, in 1963. He received the M.Sc.E.E. degree from Aalborg University, Aalborg East, Denmark, in 1987, and the Ph.D. degree from the Institute of Energy Technology, Aalborg University, in 1995.

He was with ABB-Scandia, Randers, Denmark, from 1987 to 1988. During 1988–1992 he was a Ph.D. student at Aalborg University. He became an Assistant Professor in 1992, an Associate Professor in 1996, and a Full Professor of power electronics and drives in 1998 at Aalborg University. In 2000, he was a Visiting Professor at the University of Padova, Padova, Italy, as well as becoming a part-time Programme Research Leader at the Research Center Risoe, working with wind turbines. In 2002, he was a Visiting Professor at Curtin University of Technology, Perth, Australia. His research areas are power electronics, static power converters, ac drives, switched reluctance drives, modeling, characterization of power semiconductor devices and simulation, wind turbines, and green power inverters. He is involved in more than ten research projects with industry. Among them is the Danfoss Professor Programme in Power Electronics and Drives. He is the author or coauthor of more than 300 publications in his research fields including the book including the book *Control in Power Electronics* (New York: Academic, 2002).

Dr. Blaabjerg is a Member of the European Power Electronics and Drives Association and of the Industrial Drives, Industrial Power Converter, and Power Electronics Devices and Components Committee Committees of the IEEE Industry Applications Society. He is an Associate Editor of the IEEE TRANSACTIONS ON INDUSTRY APPLICATIONS, IEEE TRANSACTIONS ON POWER ELECTRONICS, *Journal of Power Electronics*, and the Danish journal *Elteknik*. He has been active in the Danish Research Policy for many years. He became a member of the Danish Academy of Technical Science in 2001. He served as a Member of the Danish Technical Research Council during 1997–2003, and from 2001–2003 he was its Chairman. He received the 1995 Angelos Award for his contribution to modulation technique and control of electric drives and an Annual Teacher Prize from Aalborg University, also in 1995. In 1998, he received the Outstanding Young Power Electronics Engineer Award from the IEEE Power Electronics Society. He has received four IEEE Prize Paper Awards during the last five years. In 2002, he received the C. Y. O'Connor Fellowship from Perth, Australia, and in 2003, the Statoil Prize for his contributions to power electronics. He also received the Grundfos Prize in 2004.